Structural Properties of Nanostructured NiO Thin Films Prepared by Spray Pyrolysis Technique

Dahbi Laid[1,*], Zaouche Chouaieb[2], Benkrima Yamina[3], Gahtar Abdelouahab[4]

[1]Teacher Education College of Setif, Messaoude Zeghar, Algeria.

[2]Material Sciences Department, Faculty of Science, University of Biskra, 07000 Biskra, Algeria.

[3]Department of Exact Sciences, ENS Ouargla, Algeria.

[4]Department of biology, Faculty of sciences, University Elchahid Hamma Lakhder, 39000 El Oued, Algeria.

[*]Corresponding author: l.dahbi@ens-setif.dz

Abstract

In this work, nickel oxide thin films was fabricated on glass substrate at different temperature by spray pyrolysis technique. The NiO layers were obtained with different molar concentrations. The NiO thin films were crystallized with a cubic structure that can be related to obtaining peaks in the XRD diffraction of NiO thin films. The nanostructures NiO thin films were studied by the XRD patterns with two peaks at 2θ = 37.5° and 43.3° corresponding to (111) and (200) plans of NiO phase structure. The NiO thin films prepared at a concentration of C=0.05 mol/l at a temperature T= 500°C has the largest value of lattice parameter 0.42153nm. We obtained the least thickness of NiO thin films and the least crystallite size which is 11nm for the prepared thin films at a molar concentration of C=0.1 mol/l at a temperature T= 400°C.

Keywords: Nickel oxide, Thin films, Spray pyrolysis technique, Structural Properties.

Tob Regul Sci. ™ 2023;9(1): 2819-2831
DOI: doi.org/10.18001/TRS.9.1.193

1. Introduction

In the latest research, the nickel oxide (NiO) was found in the cubic structure with a lattice parameter (a= 0.4186 nm) [1]. NiO is forming of nickel metal and oxygen element, it is a p-type of semiconducting nature. NiO was used in a variety of technology such as optoelectronic devices and gas sensing [2,3] due to having a good structure crystallinity, good electrical conductivity and high transparency in the visible region. The optical band gap of NiO thin films varied between 3.6 to 4 eV [4]. However, the NiO thin films can be used in various applications due to the simplicity of synthesis such as solar cells [5], chemical sensors [6], photo detectors [7], electro

chromic minors [8], organic light-emitting diodes [9], UV detectors [10], vans parent diodes [11], and defrosting windows [12].

Table 1 shows the physical and chemical properties of NiO material, it is found that the NiO has a high solubility in water with a refractive index of 2.18. The NiO as a thin film was studied on verities of substrates with chemical and physical methods; it was used to improve the structural optical and electrical properties. The pulsed laser deposition [13], chemical vapor deposition [14], electrochemical deposition [15], abeam evaporation [16], anodic deposition [17], electroless bath deposition [18] sputtering [19], chemical vapor deposition [20] and spray pyrolysis techniques [21-23], are used to prepare the NiO thin films, the spray techniques also were favorites with comparing by others methods due to the simple deposition and best cost.

Table 1. Summary of the basic physical and chemical properties of NiO material.

Property	Value
Appearance	Green crystallinesolid
Molecular mass	74.69 g/mol
Density (N)(cm^3)	6.67 g/cm3
Latticeparameter (a)	0.4186 nm
Stable Phase at 300 K	3.1-4.3 eV
Conductivity σ $(\Omega cm)^{-1}$	1.5×10^{-3}
Melting Point	1995°C
Refractive Index	2.18
Band Gap Energy (Eg)	3.6-4.0 eV
Solubility in water μ ($cm^2/V.s$)	0.1-1
a	4.75 Å
b	11.77 Å
c	8.44Å
B	93° 36'

The mean objective of this research is to study the structural properties of NiO thin films based on past research. In this work; we have proposed a review of original research to nanostructured NiO prepared by spray techniques.

2. Structural Properties of NiO Thin Films

The NiO thin films were crystallized with a cubic structure that can be related to obtaining peaks in the XRD diffraction of NiO thin films. The nanostructures NiO thin films were studied by the XRD patterns with two peaks at 2θ = 37.5 and 43.3 corresponding to (111) and (200) plans

of NiO phase structure. The NiO thin films were deposited with various conditions such as precursor molarity, substrate temperature, film thickness and doping level.

Ahnet al [24] deposited the NiO thin films on Pt/Ta/glass by (RF) sputtering method at 50 W RF power with 10 m Torr at 600 °C. Found that the NiO thin film has a polycrystalline nature with preferentially (111), it is high than other diffractions which indicating that the preferred orientation with (111) plan. Some authors [25-27] investigated the effect of precursor molarity on the structural property, they discussed that the high crystalline structure of NiO thin films was obtained in the film prepared with 0.1 M.

Kamel et al. [28] studied the influence substrate temperature on the structural properties spray deposition NiO thin films. In this research, the NiO thin films were deposited at different temperatures, where high then of 275°C. They found that the NiO thin films having preferential orientation along (111) direction peak, so that the deposition temperature was affected on the structural property. On the other hand, the effect of substrate temperature was investigated by various authors [29-33]. The structural properties of NiO thin films show that the high crystalline structure was improved with increasing the deposition temperature.

The influences of metal doping on the structural property of NiO thin films were developed by various techniques Na, Fe, Zn, Cu, Co, Ag, Ng, Ti, Li and Mg. Nickel oxide is a compound semiconductor of (II-VI) group of the periodic table and it has a crystalline structure of the rock salt type lattices. Each cubic unit cell has four nickel atoms and four oxygen atoms. Each nickel atom is surrounded by six oxygen atoms and each oxygen atom has six nickel atoms surrounding it. This face-centered cubic (FCC) structure has a lattice parameter of 4.1769A° at 26°C. The nickel distance is 2.9518Å for a cubic cell (α=60° and a=4.1769Å)[34-35].

NiO thin films also were studied as a function of films thickness by some method, Karaduman et al. [36] prepared the Nanostructured NiO thin films with different film thickness; it is prepared using by SILAR Method to use as gas sensing application. NiO thin films in this work having a high crystalline structure with cubic structure, which was achieved in the film prepared with 330 nm, it is (200) phase. However, the film prepared others film thicknesses have good crystallinity. We have discussed that the film thickness were affected on the structural property, it is achieved with 400 to 500 nm and was found by [37-41].

Table 2. The preferred orientation and thickness of various deposited NiO thin films.

S.N.	Condition	Preferred orientation	Thickness of NiO films	Ref.
Li-NiO	420°C	(111)	19 (μm)	[42]
NiO-Ag	400°C	(200)	13 (nm)	[43]

	Ni : 42.13 % atomic Ag: 11.06 % atomic O: 47.13 % atomic P : 5.10^{-4} mbar			
NiO-B	NiO:97 % B:3% 400°C C = 0.1 M	(111)	15.2 (nm)	[44]
NiO	C = 0.5 M T=500°C	(111)	275 (nm)	[45]
NiO	C = 0.5 M T=500°C Precusar = 10 Ml	(111)	2.5 (µm)	[46]
$Co_xNi_{1-x}O$	C =0.1 M T = 573°K X = 0.15 Nozzl = 28 cm	(111)	78.55 (µm)	[47]
NiO:8Li	C = 1 M T = 600°C	(111)	48 (nm)	[48]
NiO:8Li	C = 1 M T = 400-300°C	(111)	200 (nm)	[49]
NiO	Ni = 58.80 w % O = 22.26 w % C = 18.93 w % T = 470°C	(111)	250 (nm)	[50]

NiO	T = 300°C C = 0.03 M	(111)	1000 (nm)	[51]
NiO	T = 360°C C = 0.1 M	(111)	90 (nm)	[52]
NiO	T = 460°C C = 0.2 M	(200)	0.44 (µm)	[53]
NiO_{1-x} Zn_X	T = 623°K C = 0.1 M X = 0.05	(111)	240 (nm)	[54]
NiO	T = 350°C C = 0.75 M	(220)	390 (nm)	[55]
NiO	T = 450°C C =0.01	(200)	80 (nm)	[56]
NiO-Cu	T = 1737°F Cu = 16.17 at%	(111)	100 (nm)	[57]
$(NiO)_{1-x}(ZnO)_x$	T = 400°C C = 0.05 M X = 0.25	(111)	0.3 (µm)	[58]

2.1. Preferred Orientation

The microstructure of thin films can be evaluated by X-ray diffraction, e.g. using the Bragg-Brentano geometry. I find that in a poor vacuum all the diffraction peaks for a given system are present, i.e. the film is "powder-like", as reported for instance in the JCPDS files; even amorphous films can be obtained, if the vacuum is "bad" enough. However, in a very good vacuum" preferred growth" is observed; in the extreme case only one family peak is present; for instance, only the (111) and (222) peaks are observed for f.c.c (see Table 2). Elements, like Al or Au. This is due to the fact that the (111) oriented surface is the lower energy ones. Very good vacuum means that the atoms can migrate on the surface long enough to find their lower energy

position before the arrival of another atom I used the term "preferred growth" instead of the "preferred orientation" because the latter is an artifact experienced when preparing a sample by computation of powder, and is caused by the relative arrangement of the various crystallites; by contrast the "preferred growth" has a pregnant physical meaning, as described above. The vacuum is "good" when thermodynamics dominates over kinetics: the probability of the growth of an already nucleated grain is larger than the probability of the nucleation of a new grain [59].

2.2. Grain Size

Particle size, also called grain size (see Table 3), refers to the diameter of individual grains of sediment, or the lithified particles in classic. The term may also be applied to other granular materials. This is different from the crystallite size, which refers to the size of asingle crystal inside a particle or grain.

A single grain can be composed of several crystals. Granular material can range from very small colloidal particles, through clay, silt, sand, gravel, and cobbles, to boulders[60].

Table 3. The grain/crystallite size of the various NiO films deposited at the different conditions.

S.N.	Condition	Grain \ Crystallite size (nm)	Technique	Ref
NiO-Ag	400°C Ni : 42.13 % atomic Ag: 11.06 % atomic O: 47.13 % atomic P : 5.10^{-4} mbar	11.00	XRD	[43]
NiO-B	NiO:97 % B:3% 400°C C = 0.1 M	30.00	XRD	[44]
NiO	C = 0.5 M T=500°C	1100	XRD	[45]
NiO	C = 0.05 M T=450°C	20.00	XRD	[22]

$Ni_{1-x}Zn_xO$	C = 0.05 M T=480°C	13.47	XRD	[35]
NiO	C = 0.5 M T=500°C Precusar = 10 mL	73.62	SEM	[46]
$Co_xNi_{1-x}O$	C =0.1 M T = 573°K X = 0.15 Nozzl = 28 cm	124	XRD	[47]
NiO:8Li	C = 1 M T = 600°C	17.7	SEM	[48]
NiO:8Li	C = 0.1 M T = 400-430°C	20	SEM	[49]
NiO	C = 0.2 M T = 470°C	50	XRD	[50]
NiO	T = 300°C C = 0.03 M	20	SEM	[51]
$NiCo_2O_4$	T = 300° C = 0.1 M	10	XRD	[61]
NiO	T = 360°C C = 0.1 M T_a = 30 min	116	XRD	[52]
NiO	T = 460°C C = 0.2 M	350	XRD	[53]

$NiO_{1-x}Zn_X$	T = 623°K C = 0.1 M X = 0.05	18.75	XRD	[54]
NiO	T = 350°C C = 0.75 M	12.82	AFM	[55]
NiO	T = 450°C C =0.01	92	XRD	[56]

2.3. Lattice Parameter

The lattice constant (see Table 4), or lattice parameter, refers to the physical dimension of unit cells in a crystal lattice. Lattices in three dimensions generally have three lattice constants, referred to as a, b, and c. However, in the special case of cubic crystal structures, all of the constants are equal and we only refer to a. Similarly, in hexagonal crystal structures, the a and b constants are equal, and we only refer to the a and c constants. A group of lattice constants could be referred to as lattice parameters. However, the full set of lattice parameters consist of the three lattice constants and the three angles between them.

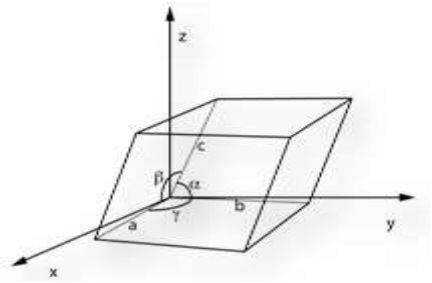

Figure 1. Unit cell definition using parallelepiped with lengths a, b, c and angles between the sides given by α, β, γ [hk1] [62]

For example, the lattice constant for a diamond is a = 3.57 Å at 300 K. The structure is equilateral although its actual shape cannot be determined from only the lattice constant. Furthermore, in real applications, typically the average lattice constant is given. Near the crystal's surface, the lattice constant is affected by the surface reconstruction that results in a deviation from its mean value. This deviation is especially important in nanocrystals, since the surface to nanocrystal core ratio is large [62]. As lattice constants have the dimension of length, their SI unit is the meter. The lattice constants are typically on the order of several angstroms (i.e. tenths of a nanometer). The lattice constants can be determined using techniques such as X-ray

diffraction or with an atomic force microscope. The lattice constant of a crystal can be used as a natural length standard of the nanometer range.

In epitaxial growth, the lattice constant is a measure of the structural compatibility between different materials. Lattice constant matching is important for the growth of thin layers of materials on other materials; when the constants differ, strains are introduced into the layer, which prevents the epitaxial growth of thicker layers without defects [62].

2.4. Mean Strain

In general terms, the strain is a macroscopic measure of deformation. Truesdell and Toupin, in their famous Classical Field Theories review article in Handbuch der Physik, introduce the concept as "The change in length and relative direction occasioned by deformation are called [63], loosely strain (see Table 4).

The concept is indeed loose until some additional qualifiers are called upon to render the matter more specific.

Table 4.The grain/crystallite size of the various NiO films deposited at the different.

S.N.	Condition	Lattice parameter a (nm)	ε ($L^{-2}m^{-4}$)	Ref
NiO	C = 0.5 M T=500°C	0.42153	--	[64]
NiO	C = 0.2 M T=400°C	0.41903	$6.39\ 10^{-3}$	[45]
$Ni_{1-x}Zn_xO$	C = 0.05 M T=480°C	0.41752	--	[35]
NiO-Li	C = 0.1 M T=460°C	0.4186	--	[65]
$Ni_{(1-x)}Mn_xO$	C = 0.2 M T=380°C	0.4173	--	[66]

3. Conclusion

Nickel oxide (NiO) has attracted a great deal of attention due to its wide direct band gap of (3.6-4.2 eV), which exhibits p-type conductivity. Stoichio metric NiO is an insulator with a resistivity of the order of $10^{13}\Omega$.cm at room temperature. NiO is one of the most important oxide materials due to its excellent chemical stability and durability, low toxicity, large span optical density, low cost and good thermal stability and high stability that are similar to ZnO. NiO can be used in various potential applications such as solar cells due to the p-type semiconducting, transparent diodes, transparent transistors, displays and defrosting windows because their transparency can be used for the UV photo detectors and touch screens due to the good responsively. NiO can be produced by several techniques such as reactive evaporation, molecular beam epitaxy (MBE), magnetron sputtering technique, pulsed laser deposition (PLD), spray pyrolysis, sol–gel process, chemical vapor deposition, and electrochemical deposition. The NiO thin films were crystallized with a cubic structure. The nanostructures NiO thin films were studied by the XRD patterns with two peaks at 2θ = 37.5° and 43.3 corresponding to (111) and (200) plans of NiO phase structure. We obtained the largest value lattice parameter of NiO thin films which is 0.42153nm for the prepared thin films at a molar concentration of C=0.05 mol/l at a temperature T=500°C. The NiO thin films prepared at a concentration of C=0.1 mol/l at a temperature T=400°C has the least thickness of NiO thin films and the least crystallite size.

References

1. A. Dihaa, S. Benramache, B. Benhaoua, Optik **172**, 832(2018). Y. Adachi, N. Saito, I. Sakaguchi, T.T. Suzuki, Thin Solid Films **685**, 238(2019). S. Benramache, Y. Aoun, A. Charef, B. Benhaoua, S. Lakel, ''Inorganic and Nano-Metal Chemistry **49**(6), 177(2019).
2. R. Vinodkumar, J. Varghese, J. Varghese, S.K Saji, N.V. Unnikrishnan, Optik**174**, 274(2018).
3. D. Selvakumar, R. Vasudevan, R. Jayavel, Materials Today: Proceedings **5**(6), 14468(2018).
4. M.N. Suma, M.V.N. Prasad, V. Gaddam, K. Rajanna, M. M. Nayak, Journal of Pure Appliedand Industrial Physics **9**(1), 1(2019).
5. H.Y Lee, C.W. Lin, C.T. Lee, Journal of Alloys and Compounds **773**, 210(2019).
6. D. Dong, W. Wang, A. Barnabé, L. Presmanes, A. Rougier, G. Dong, F. Zhang, H. Yu, Y. He, X. Diao, ElectrochimicaActa **263**, 277(2018).
7. C.T. Tsai, C.T. Wang, Y.Y. Chen, P.C. Kao, S.Y. Chua, Journal of Alloys and Compounds **797**, 159(2019).
8. L. Li, Z. Liu, L. Wang, B. Zhang, Y. Liu, Ji.P. Ao, ''Materials Science in Semiconductor Processing **76**, 61(2018).
9. S. Joseph, O. N. Balasundaram, Journal of Advanced Physics **7**(6), 319(2018).
10. M. Shkir, V. Ganesh, S. AlFaify, I. S. Yahia, H. Y. Zahran, ''Journal of Materials Science: Materials in Electronics **29**(8), 6446(2018).

11. A. Charef, S.Benramache, Y.Aoun, B. Benhaoua, S.Lakel, M.Marrakchi, Journal of Nanoelectronics and Optoelectronics **14**(5), 1667(2019).
12. A. Diha, S. Benramache, L. Fellah, Journal of nano- and electronic physics **11**(3), 3002(2019).
13. S. Benramache, Y. Aoun, S. Lakel, B. Benhaoua, C. Torchi, Sādhanā**44**(26), 334(2019).
14. Y. Aoun, M. Marrakchi, S. Benramache, B. Benhaoua, S. Lakel, A. Cheraf, Materials Research **21**(2), 20170681 (2018).
15. Y. Arata, H. Nishinaka, D. Tahara, M. Yoshimoto, CrystEngComm**20**, 6236(2018).
16. L. Ghimpu, V. Suman, D. Rusnac, International Conference on Nanotechnologies and Biomedical Engineering **77**, 291(2019).
17. M.B. Cosar, Journal of Vacuum Science & Technology A **36**, 31501(2018).
18. C. Augustine, M. N. Nnabuchi, R.A. Chikwenze, F.N.C. Anyaegbunam, C. Nwosu, C.O. Dike, C.V. Ezeh, B.J. Robert, E.M. Yohanna, E.N. Taddy, Chalcogenide Letters **15**(12), 591(2018).
19. S. Akinkuade, B. Mwankemwa, J. Neln W. Meyer, Physica B: Condensed Matter **535**, 24(2018).
20. C. Zaouche, Y. Aoun, S. Benramache, A. Gahtar, Scientific Bulletin of valahia University materials and mechanics **17**(17), 27(2019).
21. C. Zaouche, L. Dahbi, S. Benramache, A. Harouache, Y. Derouiche, M. Kharroubi, H. A. Haslouk, M. A. A. Banalhag, H. M. Alkhojah, Journal of Ovonic Research **19**(2), 197(2023).
22. Y. Ahn, J. Jang, J.Y. Son, Journal of Electroceramics **38**, 100(2017).
23. J. Zhu, J. Jiang, J. Liu, R. Ding, H. Ding, Y. Feng, G. Wei, X. Huang, Journal of Solid State Chemistry **184**(3), 578(2011).
24. I. A. Dhole, Y. H. Navale, C. S. Pawar, S. T. Navale, V. B. Patil, Journal of Materials Science: Materials in Electronics **29**(6), 5675(2018).
25. E.R. Shaaban, M.A. Kaid, M.G.S. Ali, Journal of Alloys and Compounds **613**, 324(2014).
26. H.Kamal, E.K. Elmaghraby, S.A. AlicK. Abdel-Had, Journal of Crystal Growth **262**(1-4), 424(2004).
27. K. Zrikem, G. Song, A.A. Aghzzaf, M. Amjoud, D. Mezzane, A. Rougier, Superlattices and Microstructures **127**, 35(2019).
28. A. Gahtar, S. Benramache, C. Zaouche, A. Boukacham, A. Sayah, ADVANCES IN MATERIALS SCIENCE 20(3), 36(2020).
29. M. Kaur, B.K. Dadhich, R. Singh, K. Ganapathi, T. Bagwaiya, S. Bhattacharya, A.K. Debnath, K.P. Muthe, S.C. Gadkari, Sensors and Actuators B **242**, 389(2017).
30. K.O. Ukoba, T.C. Jen, 2019 IEEE 2nd International Conference on Power and Energy Applications (ICPEA), Singapore, Singapore,**171**(2019).
31. M. Tyagi, M. Tomar, V. Gupta, Materials Science and Engineering: B **240**, 147(2019).
32. I. Dhanya, B. Sasi, Journal of Coatings **213**, 981515(2013).

33. C. Zaouche, A. Gahtar, S. Benramache, Y. Derouiche, M. Kharroubi, A. Belbel, C. Maghni, L. Dahbi, Digest Journal of Nanomaterials and Biostructures**17**(4), 1453(2022).
34. I. Karaduman, T. Çorlu, M. A.Yıldırım, A. Ateş, S. Acar, Journal of Electronic Materials **46**, 4017(2017).
35. E.S. Hassan, A. A. S, A. K. Elttayef, Journal of Materials Science: Materials in Electronics **27**, 1270(2016).
36. A. M. El Sayed, Materials Research Express **6**(11), 116423(2019).
37. N. Duraisamy, A. Numan, S.O. Fatin, K. Ramesh, S. Ramesh, Journal of Colloid and Interface Science **471**, 136(2016).
38. P.S. Patil, L.D. Kadam, Applied surface science **199**(1-4), 211(2002).
39. A. Gahtar, A. Benali, S. Benramache, C. Zaouche, Chalcogenide Letters **19**(2), 103(2022).
40. P. Puspharajah, S. Radhakrishna, A. K. Arof, Journal of Materials Science **32**, 3001(1997).
41. Y.A.K. Reddy, B. Ajitha, P.S. Reddy, M.S.P. Reddy, J.H. Lee, Electronic Materials Letters **10**, 907(2014).
42. U. Alver, H. Yaykaşlı, S. Kerli, A. Tanriverdi, International Journal of Minerals, Metallurgy, and Materials **20**, 1097(2013).
43. A.A.Yadav, U.J.Chavan, Journal of Electroanalytical Chemistry **782**, 36(2016).
44. V.Gowthami, M.Meenakshi, P.Perumal, R.Sivakuma, C.Sanjeeviraja, Materials Science in Semiconductor Processing **27**, 1042(2014).
45. R. Sharma, A.D.Acharya, S. Moghe, S.B. Shrivastava, M. Gangrade, T. Shripathi, V.Ganesan, Materials Science in Semiconductor Processing **23**, 42(2014).
46. C.C. Wua, C.F. Yang, Solar Energy Materials and Solar Cells **132**, 492(2015).
47. X. Yi, W. Wenzhong, Q. Yitai, Y. Li, C. Zhiwen, Journal of Crystal Growth **167**(3-4), 656(1996).
48. A. Hakim, J. Hossain, K.A. Khan, Renewable Energy **34**(12), 2625(2009).
49. Nazari, S. Gharibzadeh, F. Ansari, B. AbdollahiNejand, M. Eskandari, S. Kohnehpoushi, V. Ahmadi, M. Salavati-Niasari, Materials Letters **190**, 40(2017).
50. R. Sharma, A.D. Acharya, S.B. Shrivastava, T. Shripathi, V. Ganesan, Optik**125**(22), 6751(2014).
51. K. Sajilal, A. M. E. Raj, Optik**127**(3), 1442(2016).
52. R.Sharma, A.D. Acharya, S.B. Shrivastava, M.M. Patidar, M. Gangrade, T. Shripathi, V. Ganesan, Optik**127**(11), 4661(2016).
53. T. Chtouki, L. Soumahoro, B. Kulyk, H. Bougharraf, B. Kabouchi, H. Erguig, B. Sahraoui, Optik**128**, 8(2017).
54. R. Romero, F. Martin, J.R. Ramos-Barrado, D. Leinen, Thin Solid Films **518**(16), 4499(2010).
55. S.C.Chen, T.Y.Kuo, Y.C.Lin, H.C. Lin, Thin Solid Films **5**19(15), 4944(2011).
56. L. Herissi, L.Hadjeris, M.S. Aida, J. Bougdira, Thin Solid Films **605**, 116(2016).
57. R. S. Kate, S.C. Bulakhe,R. J. Deokate, Journal of Electronic Materials **48**, 3220(2019).

58. N.G. Cho, I.S. Hwang, H.G. Kim, J.H. Lee, I.D. Kim, Sensors and Actuators B: Chemical **155**(1), 366(2011).
59. R.J. Deokate, R.S. Kalubarme, C.J. Park, C.D. Lokhande, ElectrochimicaActa**244**, 378(2017).
60. H.W. Shin, J.Y. Son, Ultramicroscopy**205**, 57(2019).
61. S.H. Wang, S.R. Jian, G.J. Chen, H.Z. Cheng, J.Y. Juang, Coatings **9**(2), 1(2019).
62. S. Kerli, U .Alver, H. Yaykaşlı, Applied Surface Science **318**, 164(2014).
63. S.M. Menaka, G. Umadevi, M. Manickam, Materials Chemistry and Physics **191**, 181(2017).
64. B. Kannan, R. Pandeeswari, B.G. Jeyaprakash, Ceramics International **40**(4), 5817(2014).